

Article

Propagation of Overvoltages in the Form of Impulse, Chopped and Oscillating Waveforms in Transformer Windings—Time and Frequency Domain Approach

Marek Florkowski , Jakub Furgał and Maciej Kuniewski * 

Department of Electrical and Power Engineering, AGH University of Science and Technology, al. Mickiewicza 30, 30-059 Kraków, Poland; mflorko@agh.edu.pl (M.F.); furgal@agh.edu.pl (J.F.)

* Correspondence: maciek@agh.edu.pl

Received: 26 November 2019; Accepted: 5 January 2020; Published: 8 January 2020



Abstract: This paper describes a comparison of overvoltage propagation in transformer windings. Expanding and evolving electrical networks comprise various classes of transient waveforms, related to network reconfigurations, failure stages and switching phenomena, including new sources based on power electronics devices. In particular, the integration of renewable energy sources—mainly solar and wind—as well as expanding charging and energy storage infrastructure for electric cars in smart cities results in network flexibility manifested by switching phenomena and transients propagation, both impulse and oscillating. Those external transients, having a magnitude below the applied protection level may have still a considerable effect on winding electrical insulation in transformers, mainly due to internal resonance phenomena, which have been the root cause of many transformer failures. Such cases might occur if the frequency content of the incoming waveform matches the resonance zones of the winding frequency characteristic. Due to this coincidence, the measurements were performed both in time and frequency domain, applying various classes of transients, representing impulse, chopped (time to chopping from 1 μ s to 50 μ s) and oscillating overvoltages. An additional novelty was a superposition of a full lighting impulse with an oscillating component in the form of a modulated wavelet. The comparison of propagation of those waveforms along the winding length as well as a transfer case between high and low voltage windings were analyzed. The presented mapping of overvoltage prone zones along the winding length can contribute to transformer design optimization, development of novel diagnostic methodology, improved protection concepts and the proper design of modern networks.

Keywords: transformer windings; lightning; chopped; oscillating impulse; overvoltages; modulated wavelet; non-standard voltage waveforms

1. Introduction

Reliability of electric power systems, on both transmission and distribution levels, is an actual research topic [1–12]. Transformers play a crucial role in electrical networks and belong to the class of equipment which is not quickly replaceable. The subject of the presented research is the propagation of overvoltages in the form of impulse, chopped and oscillating waveforms in transformer windings, considered both in the time and frequency domain. The experiments were performed on a distribution transformer exposed during normal operational conditions to several surge stresses in the form of full and chopped lightning as well as switching phenomena. On the other hand, the integration of renewable energy sources, such as solar and wind, and expanding charging and energy storage infrastructure for electric cars results in network reconfiguration and the immanently related propagation of transients, both impulse and oscillating, originating in power electronics devices.

Hence, transformers are subjected to the non-standardized fast transients such as resonant oscillations, which may lead to the dangerous amplification of overvoltages inside the windings [3,13]. Proper transformer grounding should also be not neglected, which in case of lightning, may result in a higher total impedance and can lead to higher transformer terminal voltages than those computed by ideal grounding [14].

The frequency domain view allowed for the determination of the bands in the spectrum prone to resonances. If the incoming transient has a frequency content related to the resonance frequency zone, then the overvoltage amplification inside a winding might occur. Such cases are analyzed in the paper for various classes of the waveforms. The amplification or attenuation of overvoltages are analyzed along the transformer winding and also from the high voltage (HV) winding to low voltage (LV) side transfer perspective. Such tests of voltage exposure and overvoltage propagation allow a check of transformer immunity and are related to both distribution and power units. In the case of power transformers, standards [15–19] also require compliance with tests based on tail chopped lightning impulse. This kind of extended testing is recommended in configurations where the transformer is protected by a spark-gap or is operating in connection to a gas insulated substation. Power transformer units for a grid above 170 kV are checked routinely applying chopped lightning impulse, usually with a time delay to chopping in the range 3 μ s and 10 μ s [15,16,20]. Presented measurements were conducted both for a full impulse and chopped one, with the time delay to chopping from 1 μ s up to 50 μ s.

Another class of transient stresses is addressed by a rectangular impulse with a variable rise time, reflecting the behavior of power equipment in response to protection devices such as surge arresters. Above tests are complemented by a superimposed configuration of waveform composed of a full lightning impulse with an oscillating component, named a modulated wavelet. Such a waveform might mimic, for example, the oscillating packet appearing at the transformer terminals, propagated by the re-strikes in circuit breakers. According to the design principles, the peak values of transient overvoltages at transformer clamps are constrained by the installed protective devices to the level suggested by the insulation coordination [1,7,21,22]. Those values are much higher than the maximum nominal voltage, thus the incoming transient containing the oscillating component below the protection level may form overvoltages inside the insulation system of high voltage equipment caused by internal resonance in the windings despite the applied surge arresters. Particularly some switching transients, generated in gas insulated substations, during power making or breaking in lines supplying the transformers, ground faults or network reconfigurations, including those originated from power electronics, having oscillating character may cause high amplitude internal overvoltages. The amplitude of the overvoltage depends on the network topology, attenuation conditions and duration of the oscillating components. Transformer windings form a complex distributed resistive-inductive-capacitive (RLC) network, reflecting various internal resonances. Hence, the internal overvoltages recorded along the winding height may vary from the proportionally attenuated incoming external transients [3,23–27]. For this reason, study on internal transient waveforms in transformers, subjected to standard and non-standard excitations, including superimposed waveforms containing oscillating components, are important for the development of more reliable transformers.

In this context, the mapping of overvoltage prone zones along the winding length can contribute to the development of proper diagnostic methodology, improved protection concepts and the proper design of modern networks.

2. Characteristic of Voltage Waveforms Applied to Transformer Winding

In order to achieve a holistic view of test transformer response to various overvoltages, the following voltage stimulus, graphically illustrated in Table 1, have been applied:

- (a) full lightning impulse,
- (b) chopped lightning impulse,
- (c) rectangular impulse with a variable risetime,
- (d) modulated wavelet, i.e., superposition of a full lightning impulse with an oscillating component.

Table 1. Characteristic of voltage waveforms applied to transformer windings.

<p>(a) Full lighting impulse t_f—Front time t_t—Time to half of wave tail</p>	
<p>(b) Chopped lighting impulse T_c—Time delay to chopping t_c—Collapse time</p>	
<p>(c) Rectangular impulse with a variable risetime t_0—Initial time t_1—End of risetime t_r—Rise time</p>	
<p>(d) Superposition of full lighting impulse with oscillating component t_f—Front time t_t—Time to half of wave tail t_{w1}, t_{w2}—Initial and end time of oscillating packet ω_w—Frequency of oscillating packet</p>	

Special attention was paid to the propagation of those overvoltages along the high and low voltage windings as well as to the inter winding transfer case, while applying the stimulus between the winding terminal and ground.

The lightning impulse waveform U_l can be described by the following double exponential function:

$$U_l(t) = U_1[\exp(-t/\tau_1) - \exp(-t/\tau_2)] \tag{1}$$

where τ_1 and τ_2 define a time constant and U_1 the magnitude. For example, in high voltage testing, for the standard lightning impulse 1.2/50 μ s the time constants correspond to $\tau_1 = 0.405 \mu$ s and $\tau_2 = 68.2 \mu$ s.

In order to design the chopped impulse U_{cl} (Figure 1a), the inverted and shifted lightning waveform U_{-ls} is add (Figure 1b):

$$\begin{aligned} U_{-ls}(t) &= -U_2 \left\{ \exp\left[-\frac{(t-T_c)}{\tau_3}\right] - \exp\left[-\frac{(t-T_c)}{\tau_4}\right] \right\} & \text{for } t \geq T_c \\ U_{-ls}(t) &= 0 & \text{for } t < T_c \end{aligned} \tag{2}$$

Delay of chopping T_c can be tuned in a broad range—in the presented paper, up to 50 μ s. In this way, a chopped lightning impulse on the front and on the tail is created. The collapse time t_c is assumed to be about 0.1 μ s. Thus, the chopped lightning impulse on the tail U_{cl_tail} , shown in Figure 1a, can be by described by equation:

$$U_{cl_tail}(t) = U_l(t) + U_{-ls}(t) \tag{3}$$

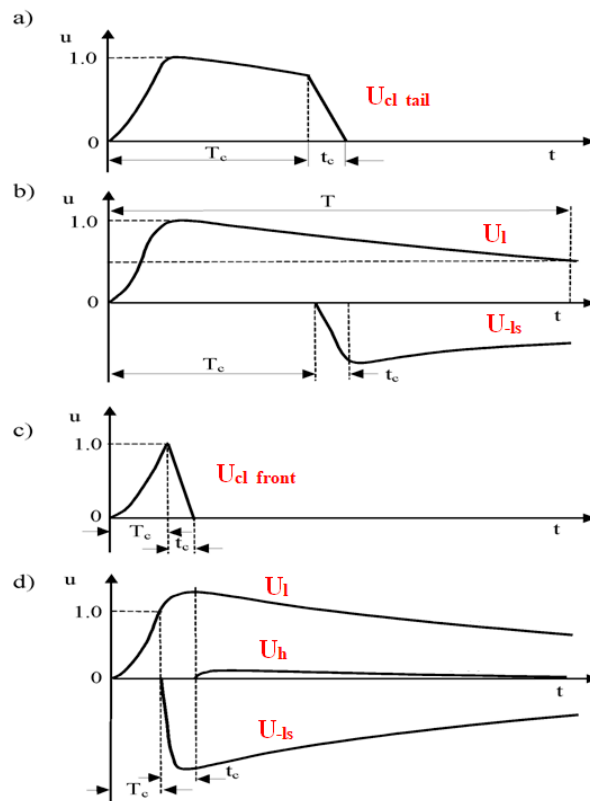


Figure 1. Illustrative formation of chopped impulse: (a) tail chopped impulse, (b) composition of component pulses for tail chopped impulse, (c) front chopped impulse, (d) composition of component pulses for front chopped impulse.

To design the impulse chopped on the front before reaching the prospective peak, the additional waveform U_h (Figure 1d) is needed, described by the following equation:

$$\begin{aligned}
 U_h(t) &= -U_3 \left\{ \exp\left[-\frac{(t-T_c-t_c)}{\tau_5}\right] - \exp\left[-\frac{(t-T_c-t_c)}{\tau_6}\right] \right\} & \text{for } t \geq T_c + t_c \\
 U_h(t) &= 0 & \text{for } t < T_c + t_c
 \end{aligned}
 \tag{4}$$

Hence, for chopped lightning impulse on the front U_{cl_front} , the superposition of full lightning impulse U_l , inverted and shifted one U_{ls} and additional waveform U_h is performed, as presented in Figure 1c,d and given by the expression:

$$U_{cl_front}(t) = U_l(t) + U_{ls}(t) + U_h(t)
 \tag{5}$$

When decaying oscillations U_{dh} follow the impulse fall at the chopping point, at a time moment $t = T_c + t_c$, the corresponding waveform component may be represented by the following expression:

$$\begin{aligned}
 U_{dh}(t) &= -U_4 \left\{ \exp\left[-\frac{(t-T_c-t_c)}{\tau}\right] \sin[\omega(t - T_c - t_c)] \right\} & \text{for } t \geq T_c + t_c \\
 U_{dh}(t) &= 0 & \text{for } t < T_c + t_c
 \end{aligned}
 \tag{6}$$

where U_4 , τ_α and ω are, respectively, the values of the magnitude, damping time constant and oscillation frequency.

To illustrate and to quantify the spectral density of full and chopped lightning impulses, the frequency analysis was performed (Figure 2), using the above presented methodology. It was based on two time-shifted pulses having inverted polarity to achieve voltage waveform with desired front time and delayed chopping moment.

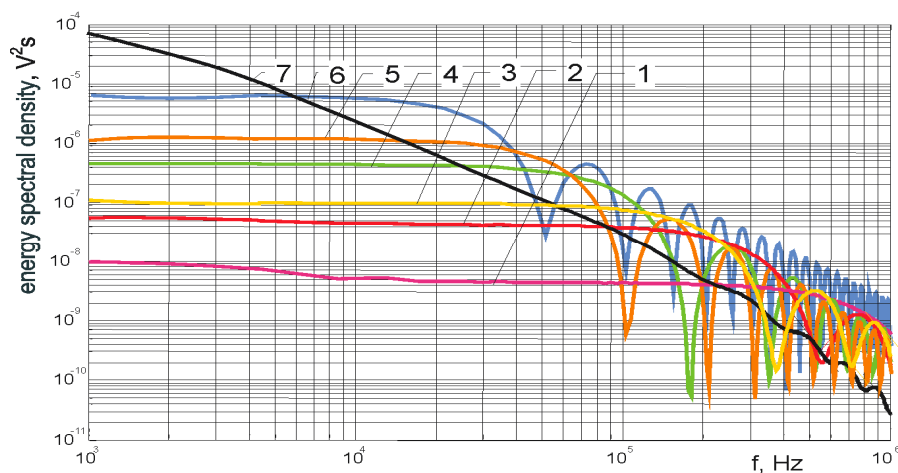


Figure 2. Spectral content of chopped and full lightning impulse (FLI). Delay time to chopping respectively: (1) 0.8 μ s, (2) 2 μ s, (3) 2 μ s, (4) 6 μ s, (5) 10 μ s, (6) 20 μ s, (7) FLI.

The chopping time significantly influences the spectral content compared with the full lightning impulse voltage, i.e., the shorter the time to chopping, the spectrum is broader but simultaneously the energy spectral density lower. This effect might have a significant implication in the case of internal transients occurring along windings lengths, while performing chopped and full lightning probe.

Another applied waveform was a rectangular impulse with a variable risetime t_r calculated between 10% and 90% of voltage slope magnitude U_5 . In the presented model, a rectangular impulse rise time is initiated at time t_0 and lasts until time moment t_1 with a slope β . Such a waveform can be described by the following expression:

$$U_r(t) = \begin{cases} 0 & \text{for } t < t_0 \\ \beta t & \text{for } t > t_0 \text{ and } t < t_1 \\ U_5 & \text{for } t > t_1 \end{cases} \quad (7)$$

The last case of a stimulus waveform U_{lw} presented in this paper refers to the superposition of a full lightning impulse U_l with oscillating component U_w , appearing at time moment t_{w1} and lasting until t_{w2} . Such a waveform with superimposed wavelet can be represented by expression:

$$U_{lw}(t) = U_l + U_w = U_l + U_6 \exp(-(t - t_{w1})^2 / \tau_w) \sin[\omega_w(t - t_{w1})] \quad \text{for } t_{w1} < t < t_{w2} \\ U_{lw}(t) = U_l \quad \text{for } t < t_{w1} \text{ and } t > t_{w2} \quad (8)$$

where τ_w and ω_w are the width and frequency of the oscillating packet.

3. Measurement Setup and Test Object

The measurement on transformer windings were performed, both in time and frequency domain, in a setup presented in Figure 3. The lightning voltage pulses were generated by a lightning stroke unit with maximum amplitude 300 V. The test waveforms with oscillating component as well as the measurements in frequency domain from 20 Hz to 2 MHz were performed using programmable function generator Tektronix type AFG310 with maximum output voltage 20 V. It is important to notice that the magnitude of the generated voltage waveforms used in experiments does not have a practical impact on measurement results. The influence of the ferromagnetic transformer core in the analysis of transients is often a subject of discussion. The contentious issue concerns the cutoff frequency of transformer core impact. Usually, referring to the investigations done by Wilcox [28], in a frequency range above several dozens of kHz, the impact of the core is neglected. Hence, in this high frequency band, the windings can be treated as linear objects and the magnitudes of applied voltage stimuli do not influence the measurements. For the acquisition of the overvoltage waveforms, an

oscilloscope Tektronix model 784D was used as in the configuration shown in Figure 3a. The frequency characteristics of the windings were obtained in the computer controlled configuration. The generator was programmed to yield the sweep in predefined frequency range (up to 2 MHz) and the corresponding response was acquired by an oscilloscope. Both the programmable function generator and the scope acting as a recorder were linked with a control computer by *GPIB-USB*. The control and analysis software was developed in *LabView™* environment from National Instruments [3,10,26,29].

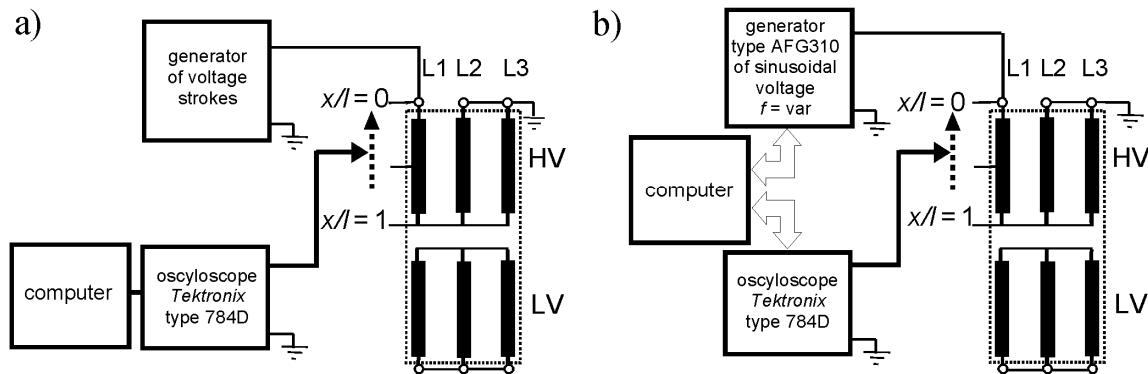


Figure 3. Measurement setup: (a) time domain measurements of overvoltages along transformer windings, (b) frequency domain and combined waveform measurements.

All experiments presented in this paper were performed on the test transformer 20 kVA 15/0.4 kV. The rated and design parameters of the experimental unit are shown in Table 2. This kind of distribution transformer was selected on purpose to test a variety of overvoltage waveforms. Such a unit can be subjected to both full lightning and chopped lightning stroke as well as to transients containing a superimposed oscillating component due to switching operations in the network. The system reconfigurations will occur increasingly frequently in the grid as a result of connected renewable generation and expanding charging and energy storage infrastructure for e-mobility.

Table 2. Experimental transformer rated and design parameters.

Parameter	Value
S_r , (kVA)	20
U_{rHV} , (kV)	15
U_{rLV} , (kV)	0.4
number of electrical phases	3
U_z , (%)	4.2
ΔP_{Fe} , (kW)	0.11
ΔP_k , (kW)	0.53
I_0 , (%)	2.8
number of turns in the coil	810
number of coils	4
winding height l , (mm)	280
internal coil diameter d_o , (mm)	157
external coil diameter d_i , (mm)	205
coil width h , (mm)	25

The research was focused on the analysis of overvoltages occurring inside transformer high and low voltage windings as well as transferred from HV to LV side. The ground overvoltages were

measured along the HV winding, at tap x/l denoted as follows: $x/l = 0$ (corresponds to the clamp of the phase L1), $x/l = 0.2$, $x/l = 0.3$, $x/l = 0.7$), applying various stimuli waveforms from the terminal side. The access to the internal winding structure was possible through additional taps installed inside in the winding. Due to the paper limitations, certain characteristic tap positions were selected to the visualization of the voltage distributions along the windings. For evaluation purposes, both the frequency and time relationships k_o of internal overvoltages in the transformer winding are calculated using following expression:

$$k_o = \frac{u_{x/l}}{u_{0_max}} \quad (9)$$

where:

$u_{x/l}$ —measurement at tap x/l along the winding,

u_{0_max} —magnitude of external stimulus applied at winding clamps (tap $x/l = 0$ and $x/l = 1.0$).

The distributions of maximum internal winding overvoltages k_{o_max} is obtained according to the relationship:

$$k_{o_max} = \frac{u_{x/l_max}}{u_{0_max}} \quad (10)$$

where:

$u_{x/l}$ —maximum value obtained for measurement at tap x/l along the winding,

u_{0_max} —highest magnitude of external stimulus applied at winding clamps (tap $x/l = 0$ and $x/l = 1.0$).

4. Overvoltages in Frequency Domain

Determination of the winding broadband characteristics in a frequency domain allows the determination of sensitive zones and resonance frequencies [3,10,12,29]. It is well suited for analysis of the response of a transformer winding to an excitation in form of an oscillating packet of overvoltage occurring in an electrical network. The normalized frequency characteristics of overvoltages along the windings are presented in Figure 4. Depending on the excitation spectral content match with these characteristics, the stress on electrical insulation systems is obtained. From the plot one can notice characteristic frequencies, for which sinusoidal excitations are strongly amplified inside the winding. Those frequencies may fit with spectrum of incoming external overvoltages. For example (Figure 4), the overvoltage ratio in case of HV winding at frequency 12 kHz equals to 3.4 p.u. Analysis confirms, that excitation waveforms having oscillating wavelet may undergo amplification inside transformer winding because of resonance phenomena, especially if the frequencies of the applied voltage are matching the self frequencies of the transformer winding.

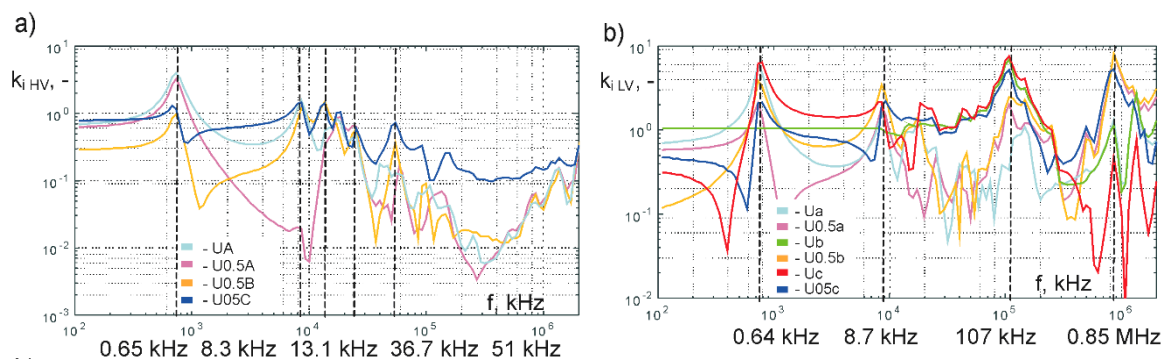


Figure 4. Frequency characteristic of terminal overvoltages and for point in half of windings and ground: (a)—HV windings, (b)—LV windings.

From the frequency characteristics of overvoltages in HV and LV experimental transformer windings (Figure 4), one can notice, that sinusoidal voltages at resonance frequencies propagated in

transformer undergo amplification inside the windings. For example, in HV windings oscillating overvoltages reach maximum for following frequencies 0.65 kHz, 13.1 kHz, 36.7 kHz and 51 kHz and in LV windings for frequencies: 0.64 kHz, 8.7 kHz, 107 kHz and 0.85 MHz. If the resonant frequencies of the transformer is larger, then the probability of multiplication of internal overvoltages in transformers is greater. It was also observed that maximal values of oscillating overvoltages in windings occurs, practically for the same frequencies, for all phases.

In turn, an interesting case is a transfer characteristic i.e., stimuli on HV winding side and response measured at LV winding, as presented in Figure 5. Illustration of the HV to LV transfer characteristic of overvoltages for injecting the signal at HV terminal of phase A and recording response at LV winding phase “a” is shown in Figure 5a, while an analogous case reflecting HV-LV winding phase C-c is shown in Figure 5b.

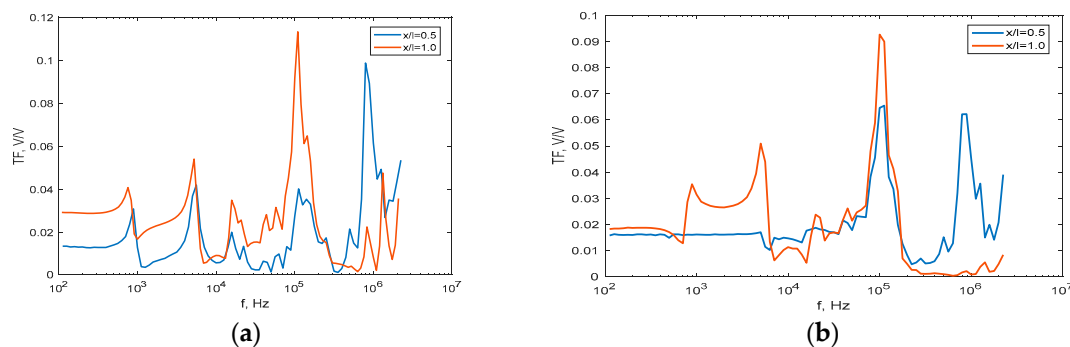


Figure 5. Transfer frequency characteristic of overvoltages at winding terminal ($x = 1.00$) and for point in half of windings and ground ($x = 0.50$): (a) injection HV windings phase A, response LV winding phase “a”, (b) injection HV winding phase C, response LV winding phase “c”.

5. Propagation of Different Waveforms in Transformer Windings in Time Domain

Overvoltages recorded in various parts of a transformer winding in response to different stimuli waveforms are presented in this section.

5.1. Full Lightning Voltage Impulse

Overvoltages measured between selected points x/l of both HV and LV winding and ground during the full lightning impulse $u_0(t)$ are presented in Figure 6a, whereas the corresponding differences of inter taps ratios are shown in Figure 6b. The magnitude of the waveform is normalized with respect to maximal value of the full lightning impulse according to formula (9). The response shapes of internal overvoltages are different comparing to the excitation applied at the external transformer clamps of one phase. For example, taking the tap at $x/l = 0.3$ in the HV winding, one can recalculate the magnitude of corresponding lightning impulse, which results in 1.04 p.u, and exceeds the impulse peak value.

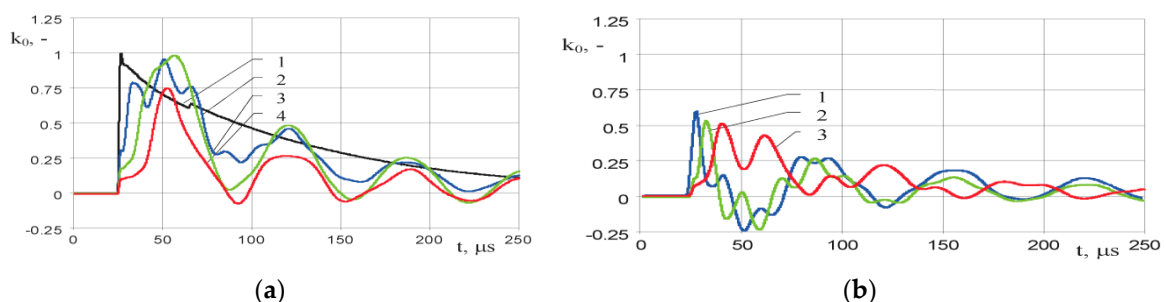


Figure 6. Measurement of overvoltages at tap x/l in (a) HV winding: (1) $x/l = 0$, (2) $x/l = 0.2$, (3) $x/l = 0.3$, (4) $x/l = 0.7$ and (b) corresponding overvoltage differences: 1— $u_{0-0.2}$, 2— $u_{0.2-0.3}$, 3— $u_{0.3-0.7}$.

5.2. Chopped Lightning Voltage Impulse

Overvoltages recorded in HV winding of 20 kVA transformer, excited by a lightning voltage impulse, were performed in a broad chopping time delay scope. The lightning impulse was chopped after time t_u from 1 μs up to 50 μs . The waveforms measured at selected taps x/l in a HV winding in response to the tail chopped lightning voltage impulse, with various chopping time delays: 2 μs , 5 μs , and 10 μs , are shown in Figure 7A and corresponding overvoltage differences in Figure 7B. The maximal values of chopped overvoltages obtained in transformer at selected taps x/l depend on time delay to chopping t_u . Increased time t_u leads to amplification of inter-winding overvoltages. Thus, time delay t_u has large influence on longitudinal overvoltage enhancement. In can be highlighted especially in a winding region being in a proximity to the transformer terminals.

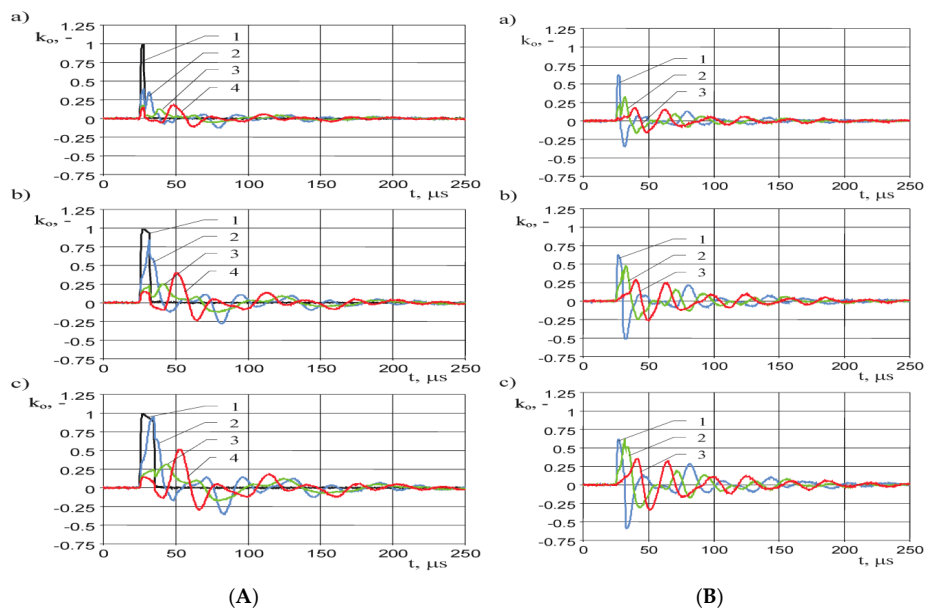


Figure 7. Measurement of overvoltages applying tail chopped lightning impulse (A) in HV winding at tap (1) $x/l = 0$, (2) $x/l = 0.2$, (3) $x/l = 0.3$, (4) $x/l = 0.7$ and (B) corresponding overvoltage differences: (1) $u_{0-0.2}$, (2) $u_{0.2-0.3}$, (3) $u_{0.3-0.7}$. Time delay to chopping t_u : (a) 2 μs , (b) 5 μs , (c) 10 μs .

The above measurements lead to the plot shown in Figure 8 representing overvoltages $k_{o-max} = f(x/l)$ between selected points and ground as well as gradients of overvoltages in HV winding of transformer excited by both full and chopped lightning voltage impulse employing time delay t_u in the range from 1 μs up to 50 μs .

The chopped voltage impulse applied to the transformer winding results according to Figure 8b in the enhanced gradients, stressing the winding electrical insulation system, especially in a proximity to the transformer clamps [6,7].

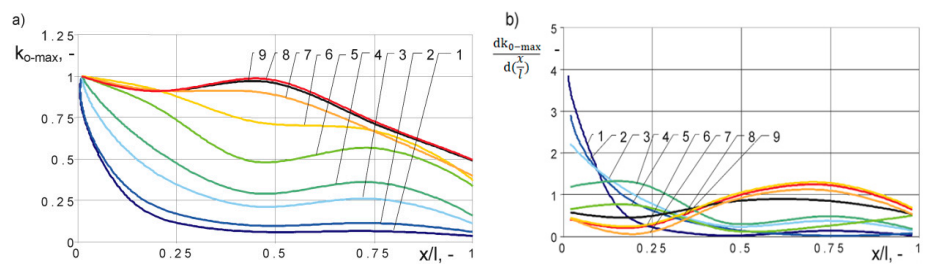


Figure 8. (a) Maximal values of overvoltages and (b) overvoltage gradient for full (FLI) and chopped lightning impulse, with time to chopping: (1) 1 μs , (2) 2 μs , (3) 4 μs , (4) 6 μs , (5) 10 μs , (6) 20 μs , (7) 30 μs , (8) 50 μs , (9) FLI.

5.3. Rectangular Voltage Impulse

In this part, transients measured in the transformer winding, excited by a rectangular impulse applied at HV clamp (tap $x/l = 0$ and $x/l = 1.0$) are presented in Figure 9.

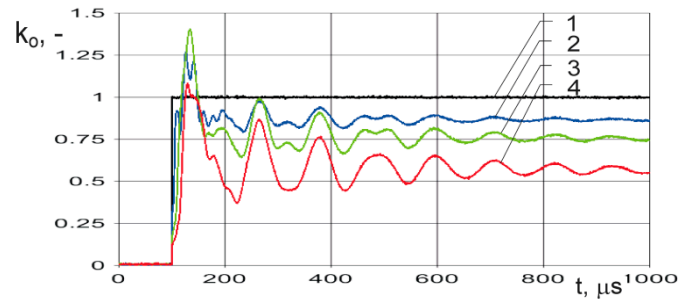


Figure 9. Overvoltages excited by rectangular impulse in the HV winding at tap: (1) $x/l = 0$, (2) $x/l = 0.2$, (3) $x/l = 0.3$, (4) $x/l = 0.7$.

Overvoltages generated inside the windings contain oscillatory components with a resonance frequency equal to 13.1 kHz. The magnitude manifests great variability, i.e., overvoltages measured at tap $x/l = 0.3$ along the winding are roughly 1.3 amplified comparing to the impulse crest value at the transformer clamp. Due to the relatively low self frequencies of HV windings, overvoltages are not sensitive to the rise time of the applied impulse, ranging from 10 ns to several hundred of nanoseconds. In turn, overvoltages generated inside the LV transformer windings in response to the rectangular voltage impulse strongly depend on rise time (Figure 10). It is possible to notice, for example, the overvoltage coefficient k_{iLV} for voltage $U_{0.5c}$ in the LV winding of phase “c” for a rise time of 10 ns is about 3.3 but for a rise time 100 ns is about 1.6. The overvoltage coefficient k_{iLV} of transient voltage U_a at the terminal of phase “a” for rise time 10 ns reach about 1.95 but for rise time of 100 ns is equal only to 0.7.

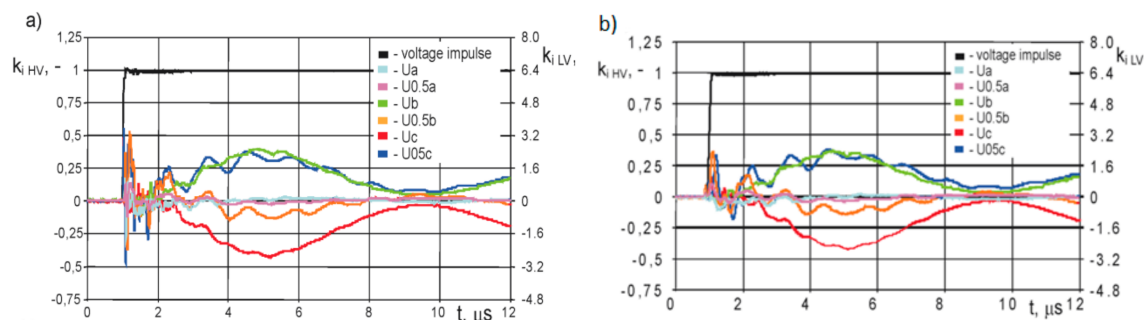


Figure 10. Overvoltages measured in transformer LV windings in response to rectangular voltage impulse with different rise times: (a) 10 ns, (b) 100 ns.

5.4. Lightning Voltage Impulse with Superimposed Oscilating Wavelet

Another class of stimulus is created by superimposed waveforms. Such an approach allows analysis of the internal overvoltages generated in the transformer winding, which result from the resonance phenomenon at impulse voltage with superimposed oscillating component, in the form of a wavelet. Thus the resultant waveform contains an aperiodic part as a lightning voltage surge and an oscillating wavelet. The oscillating frequency of the wavelet has been adjusted to the winding resonance frequencies obtained from frequency characteristics presented in Figure 4. An exemplary case of HV winding response to a lightning voltage impulse with superimposed oscillating wavelet tuned to 8.3 kHz, 13.1 kHz and 108 kHz is shown in Figure 11. One may notice the amplification of the oscillating components related to winding resonance frequencies (8.3 kHz and 13.1 kHz) inside the winding. Simultaneously overvoltages in HV windings have greater values than those generated

during action just of the lightning impulse. However, overvoltages shown in Figure 11c, excited by the lightning impulse containing oscillating component with frequency 108 kHz are not amplified in the LV winding. The wavelet frequency in this case is not matching the sharp winding resonance peak at 107 kHz.

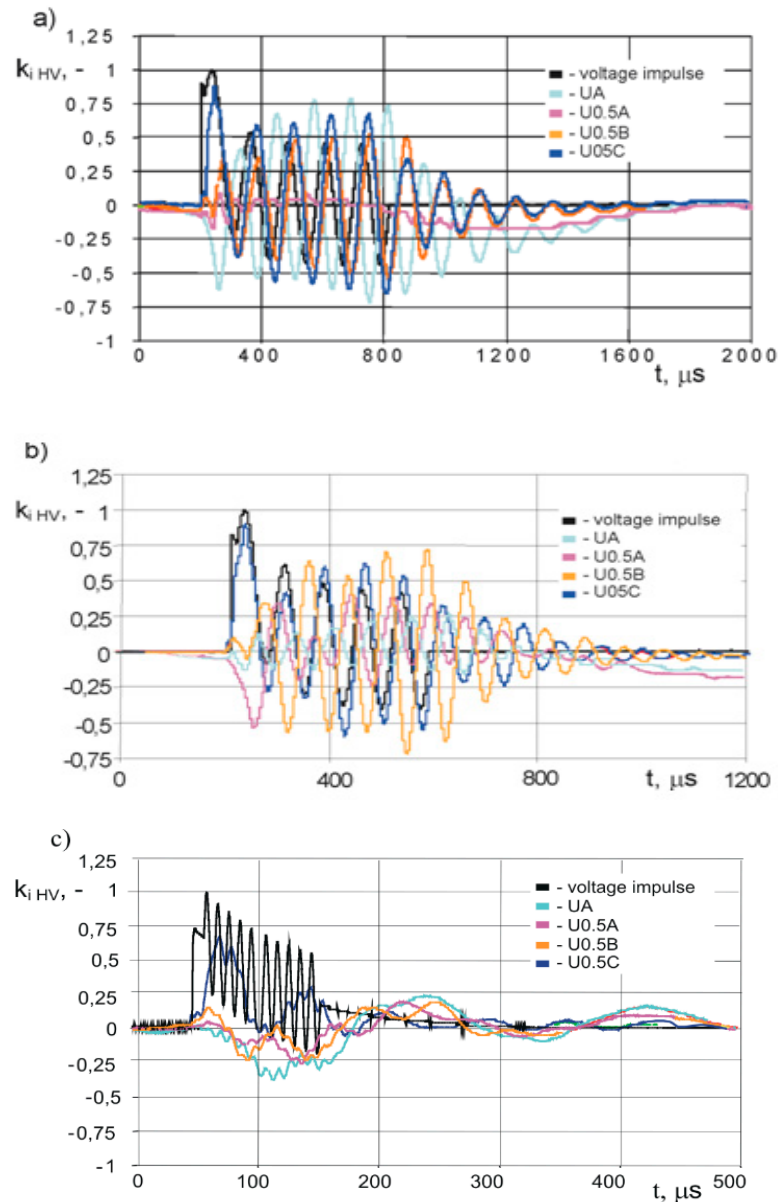


Figure 11. Response of the HV windings to lightning impulse containing oscillating components with frequency: (a) 8.3 kHz, (b) 13.1 kHz, (c) 108 kHz.

Similar measurement have been performed on LV winding, adjusting the wavelet frequency to the resonances in frequency characteristic (Figure 4), i.e., 107 kHz, 0.85 MHz. The results presented in Figure 12 also indicated strong amplification of the oscillating overvoltages in LV windings, for example in the case of frequency 0.85 MHz, the overvoltage coefficient for voltage $U_{0.5c}$ is equal to 3.4 and for voltage U_a is about 1.5. Analyzing the de-tuned case, overvoltages generated in HV winding excited by the lightning impulse containing oscillating wavelet having frequency 14.6 kHz (Figure 12c) are significantly smaller than for cases of resonance frequencies.

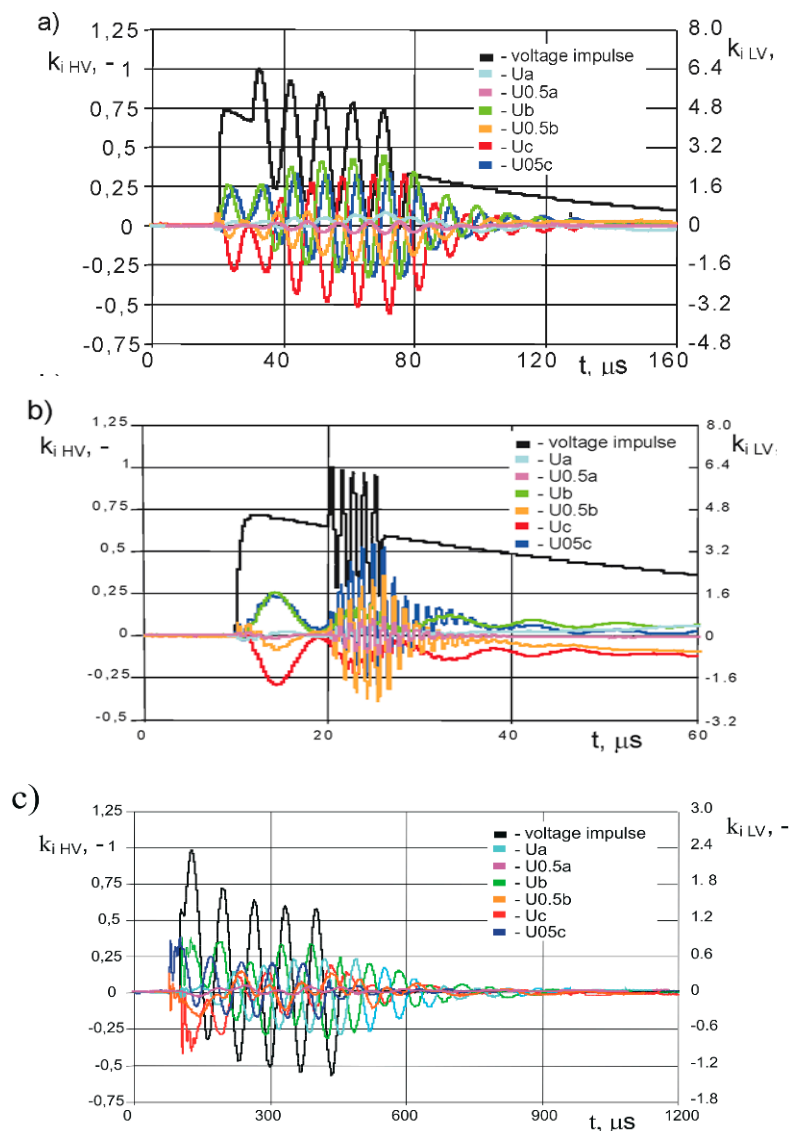


Figure 12. Response of the LV windings to lightning impulse containing oscillating wavelet. with frequency: (a) 107 kHz, (b) 0.85 MHz (c) 14.6 kHz.

6. Assessment of Overvoltages in Transformer Windings

The various applied excitation have different frequency ranges, both narrow- and broad-band. Thus observed transient overvoltages manifest different responses, applying testing voltages and waveforms, which might occur during transformer operation in a network. As a reference of transformer testing, the full lightning impulse was accepted. Power grid transients were reflected by switching and oscillating waveforms. Both cases revealed relevant distinctions of maximum overvoltages along the winding. As an assessment factor the *Time Domain Severity Factor (TDSF)* was used. The *TDSF* is evaluated according to the following expression [21,22]:

$$TDSF = \frac{U_{x/l \max}}{U_{x/l \max \text{ test}}} \quad (11)$$

where:

$U_{x/l \max}$ —highest magnitude of overvoltages occurring at tap x/l during network operation,

$U_{x/l \max \text{ test}}$ —highest magnitude of overvoltages occurring at tap x/l excited by reference voltage impulse.

The *TDSF* obtained for the experimental transformer was evaluated taking the maximum values of overvoltages yielded by testing with the standard full lightning impulse with crest value $U_{test} = 95$ kV [15]. The protection of the unit in a grid operation was considered, assuming two models of surge arresters, having different tripping and time to disconnection parameters. In the first case, the transformer has been protected by a surge arrester model SA1 rated for continuous voltage $U_c = 12$ kV, whereas the latter one is protected by model SA2 working at $U_c = 18$ kV. Both surge arresters are applied in the distinctive network operating modes, i.e., SA1 in 15 kV topologies with automatic disconnection of short circuits current to ground, whilst the model SA2 refers to the networks without automatic ground fault clearing [21,22,30]. The rated surge arrester parameters are following: for SA1 lightning protection level is $U_{lp} = 42$ kV and switching one is $U_{sp} = 31.1$ kV and for SA2 respectively $U_{lp} = 63$ kV and $U_{sp} = 46.7$ kV [30]. The dependencies, of the assessment factor $TDSF = f(x/l)$ for HV winding of experimental transformer rated 20 kVA 15/0.4 kV, were calculated and are illustrated in Figure 13.

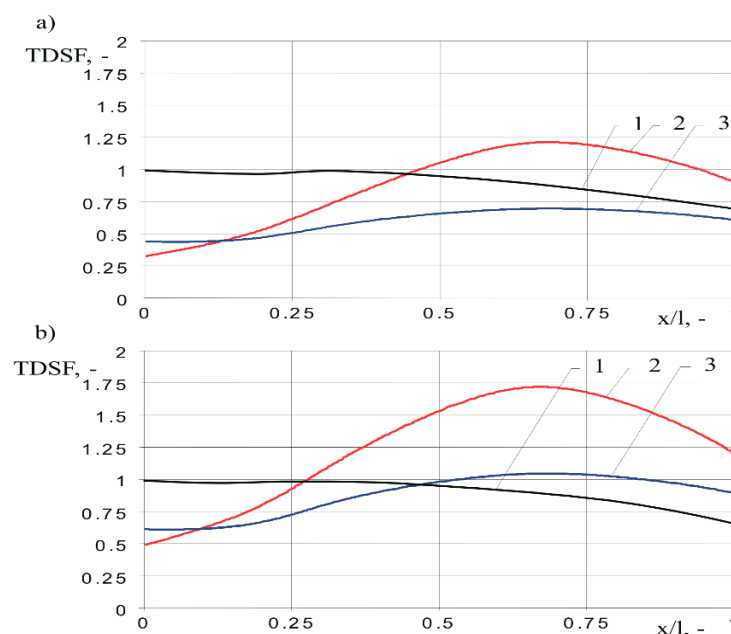


Figure 13. Assessment factor $TDSF = f(x/l)$ for HV winding excited by standard full lightning impulse $U_{test} = 95$ kV of experimental transformer protected by two models of surge arresters: (a) $U_c = 12$ kV (SA1), (b) $U_c = 18$ kV (SA2); 1—standard full lightning impulse, 2—sinusoidal wavelet with resonance frequency 13.1 kHz, 3—rectangular impulse.

The tabular summary of results of maximum overvoltages obtained for test transformer exposed to various stresses is presented in Table 3. One can notice, that overvoltages recorded at internal winding taps of transformer, in certain waveform cases, surpass magnitudes obtained at standard lightning voltage impulse tests. Maximum internal overvoltages are recorded for a sinusoidal oscillating component with the frequency matching the resonant frequency of transformer. For example, at the winding tap $x/l = 0.7$, the response to excitation of 95 kV standard lightning voltage impulse test equals to 84.6 kV.

A comparison of both cases of installed protective devices SA1 and SA2 provide quantitative illustration of transient overvoltage effects. In the case of a network equipped with SA1, with an automatic restoration after ground fault occurrence and transient excitation in the form the wavelet having the oscillating frequency 13.1 kHz (matching one of the transformer winding resonance frequencies), the measured overvoltage at the same tap was 102.6 kV. While for the experimental transformer connected to a network without automatic restoration after a ground fault occurrence, protected with SA2 device, the overvoltage at tap $x/l = 0.7$, in the response to excitation

containing the same wavelet with transformer resonant frequency, is equal to 154.1 kV. Such an analysis reflects the transformer winding sensitive zones with respect to waveform frequency content. As an extension of the presented work, further investigations on transformers with different winding topologies and voltage levels are planned. Such an approach could lead to scalable and more general methodology for assessment of overvoltages representing impulse, chopped and oscillating waveforms.

Table 3. Comparison of an impact of various waveforms on overvoltages in transformer windings.

Winding Position x/l	Reference Test Overvoltages	Overvoltages in Network Operation	
	Lightning Impulse 95 kV	Rectangular Impulse	Sinusoidal Oscillating Component
	duration: Tens of Microseconds	duration: Milliseconds	
(kV)			
Network with Automatic Fault Clearing (SA1 $U_c = 12$ kV)			
0	95.0	42.0	31.1
0.18	95.0	53.3	48.2
0.33	102.6	59.2	78.4
0.67	84.6	45.4	102.6
Network without Automatic Fault Clearing (SA2 $U_c = 18$ kV)			
0	95.0	63.0	46.7
0.18	95.0	80.0	72.4
0.33	102.6	88.8	117.7
0.67	84.6	68.0	154.1

7. Conclusions

This paper reports about propagation of various waveforms of overvoltages inside transformer winding stressing the electric insulation system. Especially highlighted are overvoltage exposures in response to a lightning voltage impulse, rectangular one and impulse containing sinusoidal oscillating component. The experiments were performed on a distribution transformer, which can be subjected in real operating conditions to such stresses in an electric network. The transformer insulation between windings and ground is exposed to the largest maximal of overvoltages during the tests with full lightning voltage impulses. The application of chopped lightning impulses, with a variable delay time to chopping does not increase the recorded transients. However, chopped lightning voltage impulses result in an enhancement of the overvoltage gradients in the electrical insulation, especially localized close to the transformer clamps. It was observed that excitation with the lightning voltage impulses chopped on tail, with a delay time above 6 μ s, does not cause an increase of overvoltage impact in experimental winding. It was noticed that attention should be paid to overvoltages containing oscillating component, especially those having the frequency close to one of the winding resonance frequencies. Knowledge of these effects broadens the knowledge about transformer immunity tests and recommendations for new designs, resistant to new classes of transients and overvoltages occurring in resilient power grid.

Author Contributions: All authors cooperated fully and equally at all stages of the presented research and during the preparation of the article. All authors have read and agreed to the published version of the manuscript.

Funding: This research received no external funding.

Conflicts of Interest: The authors declare no conflict of interest.

References

1. Joint Working Group A2/C4.39-CIGRE. *Electrical Transient Interaction between Transformers and the Power System (Part 1-Expertise, Part 2: Case Studies)*; CIGRE: Paris, France, 2014.
2. Massaro, U.; Antunes, R. Electrical transient interaction between transformers and power system—Brazilian experience. In *International Conference on Power Systems Transients (IPST2009)*; Publisher: Kyoto, Japan, 2009; pp. 1–6.

3. Florkowski, M.; Furgał, J. *High Frequency Methods for Condition Assessment of Transformers and Electrical Machines*; Publishing House AGH: Kraków, Poland, 2013; ISBN 978-83-7464-614-7.
4. Rocha, C.A.O. *Electrical Transient Interaction between Transformers and the Power System*; CIGRE-Brazil Joint Working Group JWG–A2/C4-03: Paris, France, 2008; pp. 1–6.
5. Hori, M.; Nishioka, M.; Ikeda, Y.; Naguchi, K.; Kajimura, K.; Motoyama, H.; Kawamura, T. Internal winding failure due to resonance overvoltages in distribution transformer caused by winter lightning. *IEEE Trans. Power Deliv.* **2006**, *23*, 1600–1606.
6. Lapworth, J.A.; Wilson, A. Transformer internal overvoltages caused by remote energization. In Proceedings of the 2007 IEEE Power Engineering Society Conference and Exposition in Africa-PowerAfrica, Johannesburg, South Africa, 16–20 July 2007; pp. 1–6.
7. Furgał, J. Analysis of overvoltages in windings of power transformers protected by use of metal oxide surge arresters. *Eur. Trans. Electr. Power Eng.* **2009**, *19*, 400–410. [[CrossRef](#)]
8. Shipp, D.D.; Dionise, T.J.; Lorch, V.; MacFarlane, B.G. Transformer failure due to circuit-breaker-induced switching transients. *IEEE Trans. Ind. Appl.* **2011**, *47*, 707–718. [[CrossRef](#)]
9. Holdyk, A.; Gustavsen, B. External and internal overvoltages in a 100 MVA transformer during high-frequency transients. In Proceedings of the International Conference on Power System Transmission (IPST), Cavtat, Croatia, 15–18 June 2015; pp. 1–6.
10. Florkowski, M.; Furgał, J.; Kuniewski, M.; Pająk, P. Comparison of transformer winding responses to standard lightning impulses and operational overvoltages. *IEEE Trans. Dielectr. Electr. Insul.* **2018**, *25*, 965–974. [[CrossRef](#)]
11. Srikanta Murthy, A.; Azis, N.; Mohd Yousof, M.F.; Jasni, J.; Othman, M.L.; Talib, M.A.; Das, B.P. Investigation on the Resonant Oscillations in an 11 kV Distribution Transformer under Standard and Chopped Lightning Impulse Overvoltages with Different Shield Placement Configurations. *Energies* **2019**, *12*, 1466. [[CrossRef](#)]
12. Zhang, Z.; Gao, W.; Kari, T.; Lin, H. Identification of Power Transformer Winding Fault Types by a Hierarchical Dimension Reduction Classifier. *Energies* **2018**, *11*, 2434. [[CrossRef](#)]
13. Popov, M. General Approach for accurate resonance analysis in the transformer. *Electr. Power Syst. Res.* **2018**, *161*, 45–61. [[CrossRef](#)]
14. Popov, M.; Grcev, L.; Hoidalén, H.K.; Gustavsen, B.; Terzija, V. Investigation of the Overvoltage and Fast Transient Phenomena on Transformer Terminals by Taking into Account the Grounding Effects. *IEEE Trans. Ind. Appl.* **2015**, *51*, 5218–5227. [[CrossRef](#)]
15. IEC 60076-3 Power Transformers–Part 3: Insulation Levels. Dielectric Tests and External Clearances in Air. Available online: <https://webstore.iec.ch/publication/62880> (accessed on 8 November 2019).
16. IEEE C57.98 Guide for Transformer Impulse Tests. *IEEE Power Energy Soc.* **2012**. [[CrossRef](#)]
17. Neto, E.T.W.; Lopes, G.P.; Martinez, M.L.B.; Salles, C. Chopped impulses for distribution transformers their importance for dimensioning and performance evaluation. In Proceedings of the 2014 International Conference on Lightning Protection (ICLP), Shanghai, China, 11–18 October 2014; pp. 473–478.
18. Bhuyan, K.; Chatterjee, S. Electric stresses on transformer winding insulation under standard and non-standard impulse voltages. *Electr. Power Syst. Res.* **2015**, *123*, 40–47. [[CrossRef](#)]
19. Florkowski, M.; Furgał, J.; Kuniewski, M. Propagation of overvoltages transferred through distribution transformers in electric networks. *IET Gen. Trans. Distr.* **2016**, *10*, 2531–2537. [[CrossRef](#)]
20. Munshi, S.; Roy, C.K.; Biswas, J.R. Computer studies of the performance of transformer windings against chopped impulse voltages. *IEE Proc. C* **1992**, *139*, 286–294. [[CrossRef](#)]
21. Standard EN 60071-1 Coordination of Insulation. Definitions, Principles and Rules. Available online: <https://webstore.iec.ch/publication/65606> (accessed on 8 November 2019).
22. Standard EN 60099-5 Surge Arresters. Recommendation of Selection and Use. Available online: <https://webstore.iec.ch/publication/736> (accessed on 8 November 2019).
23. Lopez-Fernandez, X.M.; Álvarez-Mariño, C. Induced transient voltage performance between transformers and VCB-severity factors and case studies. *IEEE Trans. Power Deliv.* **2015**, *30*, 1137–1144. [[CrossRef](#)]
24. Florkowski, M.; Furgał, J.; Kuniewski, M.; Pająk, P. Investigations of transformer winding response to standard full and chopped lightning impulses. In Proceedings of the 2018 IEEE International Conference on High Voltage Engineering and Application (ICHVE), Athens, Greece, 10–13 September 2018.
25. Rodrigues, R.B.; Mendes, V.M.F.; Catalão, J.P.S. Analysis of Transient Phenomena Due to a Direct Lightning Strike on a Wind Energy System. *Energies* **2012**, *5*, 2545–2558. [[CrossRef](#)]

26. Florkowski, M.; Furgał, J.; Kuniewski, M.; Pająk, P. Propagation of lightning, oscillating and non-standard impulse waveforms in transformer windings. In *The International Symposium on High Voltage Engineering*; Springer: Cham, Switzerland, 2019.
27. Xu, B.; Li, Y.; Zhao, J.; Wang, X.; Zhang, R. Simulation of propagation characteristic of ultra high frequency signals in power transformers using finite difference time domain method. In Proceedings of the 2015 5th International Conference on Electric Utility Deregulation and Restructuring and Power Technologies (DRPT), Changsha, China, 26–29 November 2015; pp. 1591–1594.
28. Wilcox, D.J.; Conlon, M.; Hurley, W.G. Calculation of self and mutual impedances for coils in ferromagnetic cores. *IEE Proc.* **1988**, *135*, 470–476. [[CrossRef](#)]
29. Yang, Q.; Su, P.; Chen, Y. Comparison of Impulse Wave and Sweep Frequency Response Analysis Methods for Diagnosis of Transformer Winding Faults. *Energies* **2017**, *10*, 431. [[CrossRef](#)]
30. Metal Oxide Surge Arresters Type POLIM-D, ABB Power Distribution. Available online: <https://new.abb.com/high-voltage/surge-arresters/medium-voltage-arresters/distribution-systems/polim-d> (accessed on 8 November 2019).



© 2020 by the authors. Licensee MDPI, Basel, Switzerland. This article is an open access article distributed under the terms and conditions of the Creative Commons Attribution (CC BY) license (<http://creativecommons.org/licenses/by/4.0/>).